# A Role for Intermediate Filaments in Determining and Maintaining the Shape of Nerve Cells□ⱽ

**Brian T. Helfand,\* Melissa G. Mendez,\* Jason Pugh,\* Claude Delsert,† and Robert D. Goldman\*‡**

\*Department of Cell and Molecular Biology, Northwestern University Feinberg School of Medicine, Chicago, Illinois 60611; and ‡Institut Français de Recherche pour l'Exploitation de la Mer , Centre de Recherche en Biochimie des Macromolécules-Centre National de la Recherche Scientifique, 1919, 34293 Montpellier, France

To date, the functions of most neural intermediate filament (IF) proteins have remained elusive. Peripherin is a type III intermediate filament (IF) protein that is expressed in developing and in differentiated neurons of the peripheral and enteric nervous systems. It is also the major IF protein expressed in PC12 cells, a widely used model for studies of peripheral neurons. Dramatic increases in peripherin expression have been shown to coincide with the initiation and outgrowth of axons during development and regeneration, suggesting that peripherin plays an important role in axon formation. Recently, small interfering RNAs (siRNA) have provided efficient ways to deplete specific proteins within mammalian cells. In this study, it has been found that peripherin-siRNA depletes peripherin and inhibits the initiation, extension, and maintenance of neurites in PC12 cells. Furthermore, the results of these experiments demonstrate that peripherin IF are critical determinants of the overall shape and architecture of neurons.

## INTRODUCTION

The cytoskeleton of vertebrate cells consists of three major types of protein networks: intermediate filaments (IF), microfilaments (MF), and microtubules (MT). Intermediate filaments are the most diverse of the three because they are encoded by >65 genes, making the IF superfamily one of the 100 largest in the human genome (Hesse *et al.*, 2001). These genes are developmentally regulated, resulting in the cell type-specific expression of IF. This is clearly evident in the nervous system, where at least seven different IF proteins are expressed, ranging from the complex neurofilament (NF) heteropolymers composed of the type IV triplet proteins NF-L, NF-M, and NF-H, to the simpler homopolymers of the type III IF protein peripherin (Leung *et al.*, 1998). Peripherin forms the major IF system of peripheral and enteric neurons, and it is abundantly expressed in PC12 cells, a widely used model for studies of peripheral neurons (Parysek and Goldman, 1987; Leonard *et al.*, 1988; Portier *et al.*, 1983a,b).

One of the hallmarks of mature or terminally differentiated neurons is their remarkable shape, highlighted by extremely long cytoplasmic processes such as axons. The initiation, extension, and maintenance of axons involve the coordinated interactions of different cytoskeletal proteins (Mueller, 1999; Dickson, 2002). To date, only MT and MF have been considered essential for growth cone activity and axon outgrowth (Letourneau, 1996). In contrast, the contribution of neural IF to these processes has not been defined.

The expression patterns of neural IF are highly correlated with different phases of axonal development. Type III IF, such as peripherin and vimentin, are present throughout early stages of outgrowth, and later type IV NF triplet proteins are expressed as axons reach maturity (Cochard and Paulin, 1984; Troy *et al.*, 1990a). In mature neurons, NF appear to be major determinants of axon caliber, and thus conduction velocity (Lasek *et al.*, 1983; Hoffman *et al.*, 1987). However, little is known about the functions of the type III IF in either developing or mature neurons. Based on their presence in early development, it is possible that Type III IF play a role in the initiation, outgrowth and maintenance of axonal structure and shape in both cultured neurons and neurons in situ. For example, in the case of PC12 cells, it has been shown that peripherin expression is significantly increased following the induction of neurite outgrowth by nerve growth factor (NGF; Aletta *et al.*, 1988; Aletta *et al.*, 1989; Leonard *et al.*, 1987). This is accompanied by the rapid formation of motile non-filamentous peripherin particles and short filament (or squiggles; Prahlad *et al.*, 1998). These two structural forms, thought to be prescursors to long IF, are found in all regions of growing neurites, including the central and peripheral domains of growth cones (Helfand *et al.*, 2003). Peripherin expression has also been correlated with the initiation and outgrowth of axons that take place within the developing nervous systems of vertebrate animals (Gervasi *et al.*, 2000; Troy *et al.*, 1990b; Undamatla and Szaro, 2001). Injured peripheral neurons in situ also show significant increases in peripherin IF expression during ax-

onal regeneration, while at the same time NF protein expression decreases (Oblinger *et al.*, 1989b). The resulting regenerating peripherin-rich axons are of notably smaller diameter relative to mature axons. Once outgrowth is completed, NF triplet proteins return to their normal levels as peripherin expression is down regulated and the mature axon caliber is re-established (Hoffman *et al.*, 1985). Based upon these observations, it appears likely that peripherin is involved in the initiation and outgorwth of axons.

Recently, the use of small interfering RNA (siRNA) to silence the expression of gene products has produced remarkable new insights into the functions of specific targeted proteins in mammalian cells (Elbashir *et al.*, 2001; Shi, 2003). In this study, we use siRNA to determine the effects of peripherin IF depletion on various parameters related to the shape and form of PC12 cells including the initiation, outgrowth, and maintenance of neurites.

## MATERIALS AND METHODS

### Cell Culture

Stock cultures of rat PC12 cells were maintained in complete medium (CM: DMEM (Invitrogen, Carlsbad, CA) containing 10% calf serum, 1 mM sodium pyruvate, and 50 U of penicillin and 50 mg/ml streptomycin) at 37°C as described previously (Helfand *et al.*, 2003). For some siRNA studies, cells from stock cultures were transferred to laminin (Roche Diagnostics, Indianapolis, IN)-coated coverslips (Fisher Scientific, Pittsburgh, PA) and grown in the presence of differentiation medium [DM; DMEM containing 5% calf serum, 1 mM sodium pyruvate, 50 U of penicillin and 50 mg/ml streptomycin and 30 ng/ml NGF (Roche Diagnostics) (for details, see Helfand *et al.*, 2003).

### Antibodies

Antibodies used in these studies included rabbit anti-peripherin (Helfand *et al.*, 2003), anti-vimentin 314 (Helfand *et al.*, 2002), and anti-keratin 8 and 18 (Yoon *et al.*, 2001). Mouse monoclonal anti-NF-L (Sigma-Aldrich, St. Louis, MO), anti-NF-M (Sigma-Aldrich), anti-NF-H (Sigma-Aldrich), anti-$\beta$-tubulin (TU 27B; provided by Dr. Lester Binder, Northwestern University, Chicago, IL), anti-human actin (Accurate Chemical & Scientific, Westbury, NY), and a rat monoclonal anti-$\alpha$-tubulin (Serotec, Oxford, United Kingdom) were also used. In some experiments, rhodamine conjugated or Cy5-conjugated phalloidin (Molecular Probes, Eugene, OR) was used to detect actin by fluorescence microscopy. Fluorescein isothiocyanate-, lissamine-rhodamine-, and Cy5-conjugated goat anti-mouse and anti-rabbit IgG (Molecular Probes) were used for indirect immunofluorescence. Peroxidase-conjugated goat anti-rabbit and anti-mouse IgG (Kirkegaard and Perry Laboratories, Gaithersburg, MD) were used for immunoblotting.

### Immunofluorescence and Image Analysis

PC12 cells were rinsed in PBS and fixed in either methanol (Mallinckrodt; $-20°C$) for 4 minutes or 3.7% formaldehyde (Tousimis) at room temperature for 5 minutes. Cells were then processed for indirect immunofluorescence as previously described (Helfand *et al.*, 2003).

Images of fixed, stained preparations were taken with a Zeiss LSM 510 microscope (Carl Zeiss, Inc.) equipped with a 40X oil immersion (1.3 NA, plan-Neofluor lens) and a 100X oil immersion (1.4 NA, plan-apochromatic lens; Helfand *et al.*, 2003).

### Half-life Studies

PC12 cells were grown in the presence of either CM or DM for 2 days prior to incubating with methionine and cysteine-free DMEM for 1 hour. All cells were then incubated with [$^{35}$S] methionine (0.2 mCi/ml in methionine-free DMEM) for 4 hours. Radioactive medium was removed and the cells were washed three times with non-radioactive media, and then fresh CM or DM was added. Cells were harvested at 0, 24, 36 and 48 hours time points. At each time point, cells were washed three times with PBS and collected in lysis buffer. PBS containing cell lysates was then centrifuged at 10,000xg in a tabletop centrifuge (Beckman R centrifuge). The pellet was incubated in IF lysis buffer (Starger and Goldman, 1977; PBS containing 1% Triton X-100, 500 mM KCl, 2 mM MgCl$_2$, 0.5 mg/ml DNase 1, and 2 mM PMSF) for 10 minutes at room temperature and centrifuged at 10,000xg (Beckman R centrifuge). The amounts of protein present in the total cell lysate, supernatant and IF-enriched pellet fractions were determined by Bradford (BioRad) analysis. The pellet fractions were sonicated into Laemmli buffer (Laemmi, 1970) and 4 $\mu$g of protein from each time point was loaded per lane and analyzed by SDS-PAGE and immunoblotting. The levels of [$^{35}$S] methionine incorporated

into peripherin were determined by autoradiography. Densitometric scanning of autoradiographs was performed on a phosphoimager (Molecular Dynamic Storm 860) and analyzed using the ImageQuant program (version 5.0).

### siRNA Studies

Peripherin-siRNA was synthesized using the Silencer siRNA construction kit (catalog no. 1620; Ambion, Austin, TX). To this end, a target sequence was identified by first scanning the length of the *Rattus norvegicus* peripherin cDNA sequence for a series of nucleotides that initiated with two sequential adenosine residues. The following DNA template and its complementary antisense sequence were then used as primers to make double-stranded peripherin-siRNA: aagagctacaggagctcaacg (base pairs 325–346; accession no. AF031878). A second peripherin siRNA (peripherin-siRNA2) using the DNA template aaggacgtggacgacgccacg (base pairs 633–653) was employed in these studies to ensure that the effects of the first peripherin-siRNA did not inhibit some unknown unrelated protein. For controls, a *Rattus norvegicus* neurofilament light chain subunit (NF-L) siRNA was made by using the base pairs aagccgagctgttggtgctgc (base pairs 427–447; Accession # NM_031783) and their complementary sequence; and an unrelated *Xenopus laevis* lamin B1 (XLB1) siRNA was made by using the following 21-mer DNA template and its complementary antisense sequence: aacaccaggatctccaggcca (base pairs 342–363; accession no. S01496). A PubMed BLAST search of the rat genome revealed that the peripherin primers were specific for rat peripherin, and there was no homologous sequence when the XLB1 DNA primers were compared with any other rat proteins.

In some experiments, cells containing siRNA were detected by labeling the siRNA with fluorescein (FAM) according to the protocol described by the Silencer siRNA labeling kit (catalog 1634; Ambion).

### Transfection

Peripherin-siRNA, or peripherin-siRNA2, at a concentration between 5 and 10 nM, was introduced into PC12 cells by OligofectAMINE (Invitrogen) delivery. Transfection was carried out under the following experimental conditions: PC12 cells were maintained in CM for up to 96 h after transfection; cells were maintained in CM for 72 h after transfection and then in DM for an additional 24 h; cells were maintained in DM for up to 96 h after transfection; and cells were grown in DM for 24 h before transfection and then maintained in DM for up to 96 h. Controls for all experiments consisted of transfecting PC12 cells with *X. laevis* lamin B1 siRNA, at a concentration between 5 and 10 nM or mock transfected with only OligofectAMINE.

### Determination of the Effects of siRNA

Immunofluorescence and immunoblotting were used to determine the effects of siRNA. For immunofluorescence studies, cells were fixed and processed at 24, 48, 72, and 96 h posttransfection as described previously (for details, see Helfand *et al.*, 2003). Phase and fluorescence images were captured simultaneously with the LSM 510 confocal microscope Carl Zeiss, Thornwood, NY). In addition, Z-section series (~0.30 $\mu$m/slice) were captured to observe the organization of peripherin in all regions of cells.
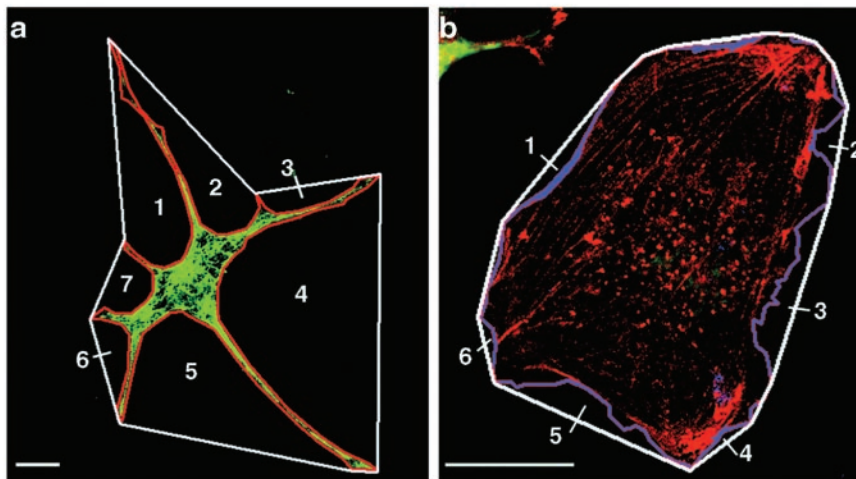
For immunoblotting experiments, PC12 cells were plated in CM or DM to a density of $6 \times 10^5$ cells/ml in 60-mm culture dishes 4 h before transfection. The cells were either transfected with peripherin-siRNA (see above) or mock transfected (controls) by using OligofectAMINE and maintained for periods up to 96 h. After trypsinization, cells were collected in either CM or DM and counted using a double Neubauer hemacytometer (Clay Adams, Parsippany, NJ). The cell suspension was pelleted on a tabletop centrifuge (200 $\times$ g, IEC HN-SII), and the medium was decanted. The pellet of cells was immediately sonicated into 200 $\mu$l of Laemmli sample buffer (Laemmli, 1970). Samples of each preparation containing the equivalent of ~200,000 cells were analyzed by SDS-PAGE (Laemmli, 1970). The separated proteins were transferred to nitrocellulose for immunoblotting (Towbin *et al.*, 1979). All antibody incubations were carried out in phosphate-buffered saline containing 5% nonfat dry milk (Sigma-Aldrich). Immunoblots were analyzed by either visualizing horseradish peroxidase-conjugated antibodies or enhanced chemiluminescence (Amersham Biosciences, Piscataway, NJ) by using radiographic film (Amersham Biosciences) as described previously (Prahlad *et al.*, 1998; Helfand *et al.*, 2003).

### Live Cell Imaging

PC12 cells were plated onto gridded coverslips (Bellco) and transfected with FAM labeled-peripherin siRNA (see above) for 72 hours and then exposed to NGF for 24 hours. Fluorescence and phase-contrast images of these cells were acquired simultaneously using the Zeiss LSM 510 microscope. Transfected cells were identified based upon the presence of the labeled siRNA. Images of transfected cells were captured every 10 seconds for time periods up to 10 minutes. After observation, cells were formaldehyde fixed and stained with peripherin antibody (see above) to verify peripherin depletion in transfected cells.

**Table 1.** Morphometric analyses of peripherin-siRNA and mock tranfected cells: form factor, process index, and process domain

| Condition | Form Factor | | | Process Index | | | Process Domain ($\mu m^2$) | | |
|---|---|---|---|---|---|---|---|---|---|
| | average | SD | p-value | average | SD | p-value | average | SD | p-value |
| **CM 96** | | | | | | | | | |
| peripherin-siRNA | 0.61 | 0.20 | < 0.001 | 3.40 | 1.46 | <0.001 | 134.15 | 113.13 | <0.001 |
| mock | 0.25 | 0.09 | | 6.30 | 1.84 | | 329.15 | 170.63 | |
| NFL-siRNA | 0.3 | 0.28 | 0.447 | 4.95 | 2.28 | 0.08 | 369.65 | 311.35 | 0.58 |
| **CM72/DM24** | | | | | | | | | |
| peripherin-siRNA | 0.59 | 0.22 | < 0.001 | 4.00 | 1.84 | <0.001 | 3023.19 | 1615.74 | <0.001 |
| mock | 0.05 | 0.03 | | 8.00 | 2.42 | | 3499.93 | 1555.92 | |
| **DM-24** | | | | | | | | | |
| peripherin-siRNA | 0.12 | 0.08 | 0.031 | 6.10 | 1.45 | 0.008 | 5309.05 | 6786.90 | 0.153 |
| mock | 0.16 | 0.10 | | 4.00 | 1.84 | | 2718.84 | 3270.68 | |
| **DM-48** | | | | | | | | | |
| peripherin-siRNA | 0.30 | 0.24 | < 0.002 | 6.55 | 2.01 | 0.959 | 1762.63 | 1846.93 | 0.050 |
| mock | 0.09 | 0.06 | | 6.50 | 3.43 | | 3569.29 | 3585.17 | |
| **DM-96** | | | | | | | | | |
| peripherin-siRNA | 0.51 | 0.20 | < 0.001 | 4.75 | 1.55 | 0.003 | 781.12 | 1125.01 | 0.0047 |
| mock | 0.05 | 0.03 | | 6.70 | 2.15 | 0.061 | 5813.48 | 7042.88 | 0.571 |
| NFL-siRNA | 0.07 | 0.07 | 0.103 | 4.00 | 5.47 | | 8168.38 | 6833.39 | |
| **DM24/DM*-24** | | | | | | | | | |
| peripherin-siRNA | 0.09 | 0.07 | 0.811 | 7.10 | 2.70 | 0.416 | 5003.34 | 4401.49 | 0.337 |
| mock | 0.10 | 0.07 | | 6.45 | 1.51 | | 3594.77 | 3659.56 | |
| **DM24/DM*-48** | | | | | | | | | |
| peripherin-siRNA | 0.17 | 0.12 | 0.007 | 7.35 | 3.07 | 0.508 | 1729.26 | 3171.71 | 0.121 |
| mock | 0.08 | 0.07 | | 6.80 | 2.26 | | 17465.96 | 46218.48 | |
| **DM24/DM*-72** | | | | | | | | | |
| peripherin-siRNA | 0.47 | 0.27 | < 0.001 | 3.20 | 2.80 | 0.003 | 1114.86 | 968.66 | <0.001 |
| mock | 0.08 | 0.05 | | 5.65 | 1.98 | | 6230.92 | 5850.84 | |



The form factor (see MATERIALS AND METHODS) was determined for both peripherin-siRNA and mock transfected PC12 cells in all experiments. The convex hull (white lines; a, b) was used to determine the process index (the number of areas between neurites and the convex hull; see for example a; numbers 1–7). In addition, the difference between the area contained within the convex hull and the area contained within the cell contour (demarcated by the red line, a; and blue line, b) was used to determine the process domain. Size bars = 10 $\mu$m. Experimental condition abbreviations: CM96 refers to transfected cells grown in the absence of NGF for 96 hours; CM72/DM24 refers to transfected cells grown in the absence of NGF for 72 hours and then exposed to NGF for 24 hours; DM-24, -48, and -72 refer to transfected cells grown in the presence of NGF for 24, 48 or 72 hours; DM24/DM*-24, -48, -72 refer to cells exposed to NGF for 24 hours, transfected and then maintained in the presence of NGF for an additional 24, 48 or 72 hours.

**Table 2.** Morphometric analyses of peripherin-siRNA and mock transfected cells: cell body length, number of processes and length of processes

| Condition | n= | Cell Body Length (μm) average | SD | p-value | Number of Processes average | SD | p-value | Process Length (μm) average | SD | p-value | Number of Neurites average | SD | p-value | Neurite Length (μm) average | SD | p-value |
|---|---|---|---|---|---|---|---|---|---|---|---|---|---|---|---|---|
| **CM 96** | | | | | | | | | | | | | | | | |
| perpherin-siRNA | 50 | 20.22 | 10.77 | < 0.001 | 1.13 | 1.98 | < 0.001 | 6.52 | 5.56 | < 0.001 | | n/a | | | n/a | |
| mock | 50 | 13.9 | 6.03 | 0.03 | 2.67 | 1.77 | 0.007 | 9.91 | 9.08 | 0.20 | | n/a | | | n/a | |
| NFL-siRNA | 20 | 16.5 | 5.02 | | 2.45 | 1.79 | | 8.22 | 4.67 | | | n/a | | | n/a | |
| **CM72/DM24** | | | | | | | | | | | | | | | | |
| perpherin-siRNA | 50 | 35.51 | 13.62 | < 0.001 | 0.4 | 1.03 | < 0.001 | 8.25 | 16.07 | <0.001 | 0.17 | 0.52 | < 0.001 | 7.16 | 17.06 | < 0.001 |
| mock | 75 | 16.39 | 7.88 | | 4.71 | 3.6 | | 20.38 | 19.18 | | 2.2 | 2.6 | | 28.32 | 22.89 | |
| **DM-24** | | | | | | | | | | | | | | | | |
| perpherin-siRNA | 50 | 21.36 | 11.14 | 0.002 | 1.22 | 1.81 | 0.003 | 25.84 | 19.74 | 0.215 | 1.32 | 1.45 | 0.157 | 28.48 | 22.26 | 0.004 |
| mock | 50 | 15.91 | 5.04 | | 1.24 | 1.3 | | 20.15 | 16.71 | | 0.94 | 1.2 | | 19.05 | 18.12 | |
| **DM-48** | | | | | | | | | | | | | | | | |
| perpherin-siRNA | 50 | 23.6 | 10.05 | 0.043 | 2.52 | 2.08 | 0.188 | 32.34 | 27.38 | 0.024 | 1.56 | 1.94 | 0.213 | 38.8 | 30.79 | 0.032 |
| mock | 50 | 20.02 | 7.16 | | 3.06 | 1.99 | | 40.43 | 33.86 | | 2.06 | 2.03 | | 48.76 | 36.27 | |
| **DM-96** | | | | | | | | | | | | | | | | |
| perpherin-siRNA | 50 | 34.82 | 14.65 | < 0.001 | 1.75 | 1.54 | < 0.001 | 12.23 | 11.86 | < 0.001 | 0.17 | 0.42 | < 0.001 | 6.89 | 15.72 | < 0.001 |
| mock | 50 | 18.95 | 6.56 | 0.005 | 2.72 | 1.03 | 0.002 | 54.92 | 42.01 | 0.69 | 2.24 | 1.1 | 0.008 | 62.77 | 41.4 | 0.70 |
| NFL-siRNA | 20 | 23.88 | 8.02 | | 4.15 | 1.35 | | 55.16 | 28.16 | | 3.5 | 2.36 | | 54.94 | 12.99 | |
| **DM24/DM*-24** | | | | | | | | | | | | | | | | |
| perpherin-siRNA | 50 | 26.33 | 10.27 | 0.164 | 3.31 | 2.66 | 0.3 | 32.13 | 25.61 | 0.018 | 1.61 | 2.1 | 0.101 | 41.12 | 30.23 | 0.035 |
| mock | 50 | 23.59 | 10.13 | | 3.92 | 3.38 | | 38.99 | 33.75 | | 2.37 | 2.75 | | 49.92 | 36.5 | |
| **DM24/DM*-48** | | | | | | | | | | | | | | | | |
| perpherin-siRNA | 50 | 18.01 | 7.73 | 0.28 | 2.84 | 2.59 | 0.616 | 40.04 | 40.95 | < 0.001 | 2 | 2.04 | 0.389 | 47.72 | 44.47 | 0.013 |
| mock | 50 | 19.93 | 9.81 | | 2.58 | 2.58 | | 60.68 | 52.36 | | 2.4 | 2.56 | | 63.19 | 52.79 | |
| **DM24/DM*-72** | | | | | | | | | | | | | | | | |
| perpherin-siRNA | 50 | 31.12 | 13.4 | < 0.001 | 2 | 1.93 | 0.002 | 14.03 | 11.02 | < 0.001 | 0.33 | 0.61 | < 0.001 | 9.48 | 16.33 | < 0.001 |
| mock | 50 | 17.16 | 6.25 | | 3.12 | 1.59 | | 50.35 | 50.2 | | 2.46 | 1.57 | | 55.18 | 45.5 | |
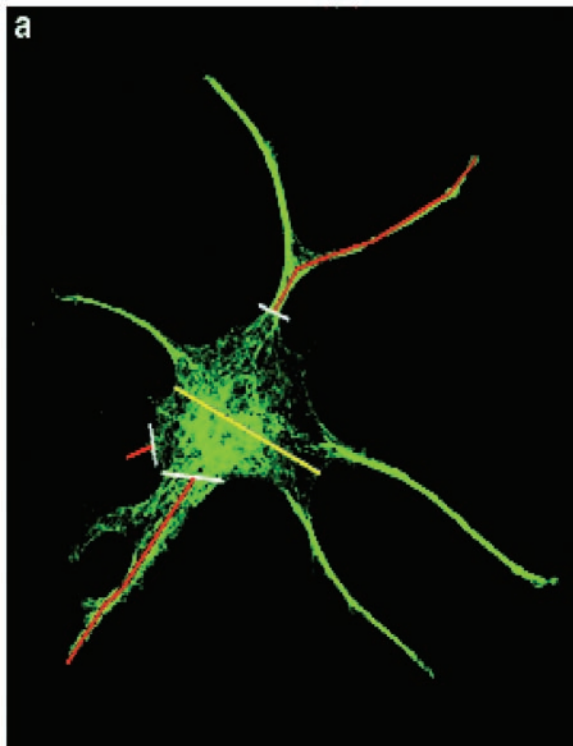


The longest axis of the cell body was used to determine the average cell body length (see MATERIALS AND METHODS and yellow line, a). Cytoplasmic processes were defined as any cytoplasmic protrusion from the cell body that was ≥2 μm in length. Neurites were defined for NGF-treated cells as any cytoplasmic process that was greater or equal to one cell body length. The process and neurite lengths were measured according to these definitions (for examples, red lines in a). White lines delineate an example of the boundaries that were used to define where a process (neurite) began. In addition, the average numbers of processes and neurites were determined. See Table 1 legend for explanations of experimental conditions. Size bar = 10 μm.
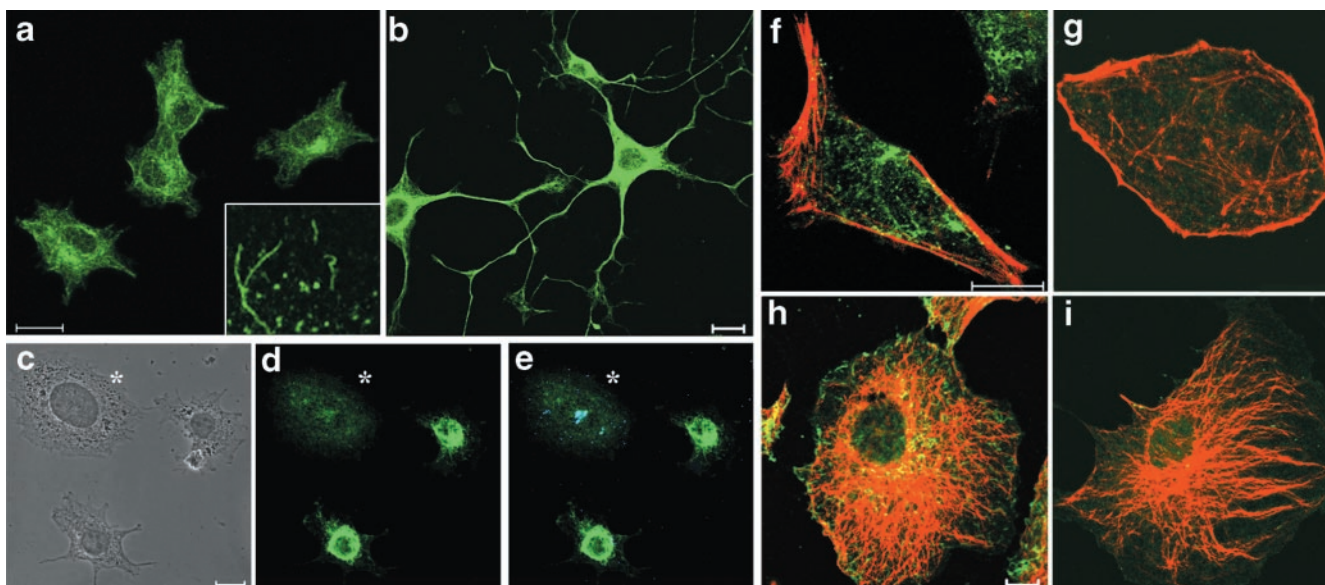
**Figure 1.** Characterization of peripherin in PC12 cells before and after treatment with siRNA. Undifferentiated PC12 cells (i.e., grown in CM) fixed and processed for immunofluorescence. (a) Peripherin (green) is present in ~100% of the cells. Inset shows a region of similar cell demonstrating the presence of particles and squiggles. (b) After exposure to NGF for 48 h, long neurites are present and the fluorescence intensity detected after processing for peripherin seems to be greatly increased relative to undifferentiated cells grown in CM. This latter observation most likely reflects the increased expression of peripherin. (c–e) PC12 cells were transfected with fluorescein-labeled peripherin-siRNA and fixed and stained with peripherin antibody after 96 h. By using confocal microscopy, 20- to 40-$\mu$m Z-section images at 0.3-$\mu$m intervals were captured to monitor the distribution of peripherin (green). (d and e) Depiction of all images in a Z-stack series. (c) A phase contrast image of the same cells demonstrates that peripherin-depleted cells (see *) spread more extensively over the coverslip (compare with the two nontransfected peripherin-containing cells that typically possess numerous cytoplasmic processes in the same microscopic field). Silenced cells contain the fluorescent siRNA (blue; see MATERIALS AND METHODS). Undifferentiated PC12 cells were transfected with peripherin-siRNA and fixed and processed for double immunofluorescence at 72 h (f and h) and 96 h (g and i) posttransfection; (f and g) peripherin (green) and actin (red); (h and i) peripherin (green) and tubulin (red). At 72 h, particles and squiggles are evident in many cells (partially silenced), whereas at 96 h, the majority of transfected cells contain no identifiable peripherin structures (extensively silenced; g and i). Peripherin siRNA had no obvious effects on the distributions of actin or tubulin (f and i). Images (a–i) were captured with a Zeiss LSM510 confocal microscope. Bars, 10 $\mu$m.

## *Morphometric Measurements and Statistical Analysis*

Two observers made all of the morphometric measurements of PC12 cells independently using the Zeiss LSM 510 imaging software (Helfand *et al.*, 2003). Phase contrast and fluorescence images were used to determine the overall shape of cells by measuring the cellular perimeter, cellular area, form factor, cellular convex hull, process domain, and process index as described previously for nerve cells (Table 1; Soll *et al.*, 1988; Kawa *et al.*, 1998; Lepekhin *et al.*, 2001). The form factor is defined as $(4\pi \times$ cellular area)/perimeter$^2$ (Soll *et al.*, 1988). Thus, perfectly round cells have a form factor of 1, whereas stellate cells have lower form factor values (Soll *et al.*, 1988). The cellular convex hull delineates the boundaries of a cell by connecting the tips of processes (for an example, see Table 1, a and b; Kawa *et al.*, 1998). After establishing the convex hull, the process index and process domains were determined (for an example, see Table 1, a and b). The process index is related to the number of cellular processes (e.g., neurites) and is defined as the number of areas contained outside of the cell contour but within the cellular convex hull (Kawa *et al.*, 1998). It has been demonstrated that the process domain correlates with process length and is defined as the difference between the areas of the cellular convex hull and the cellular area (Kawa *et al.*, 1998). All data were subsequently analyzed by Microsoft Excel, and a Student's t test (unpaired, two-tailed) was used to determine any significant differences (p < 0.005) between the parameters measured in the peripherin siRNA-transfected and control or mock-transfected cells.

More detailed analyses of PC12 cell morphology were made (for an example, see Table 2a): cell body length (defined as the length [in micrometers] of the longest longitudinal axis of the cell body that does not extend into the cytoplasmic processes), number of processes (defined as any cytoplasmic protrusion from the cell body that is ≥2 $\mu$m in length), length (in micrometers) of processes, number of neurites (defined for NGF-treated cells as any cytoplasmic process greater or equal to one cell body length), and length (in micrometers) of neurites. All of these data were analyzed as described above, except that significance was defined as p < 0.002.

## RESULTS

### *Peripherin siRNA Decreases the Level of Peripherin Expression*

When nondifferentiated PC12 cells are grown in the absence of nerve growth factor (NGF)-free culture medium (CM) (see MATERIALS AND METHODS), they seem fibroblastic in shape due to the presence of a few short cytoplasmic processes (Figure 1a). Under these culture conditions, virtually all cells (99.6%; 498/500) contain peripherin structures, mainly in the form of long IF, with lesser amounts of short IF (squiggles) and some nonfilamentous precursors (particles) distributed throughout the cytoplasm (Figure 1a, inset; Parysek and Goldman, 1987; Helfand *et al.*, 2003). A subpopulation of cells also express NF-M (~33% [99/300]; Figure 2, a–c; Parysek *et al.*, 1991), and a very small number of cells (~3% [9/300]; our unpublished data; Parysek *et al.*, 1991) express low levels of NF-L. When expressed, the NF-M is associated with a subset of peripherin IF as determined by double label immunofluorescence (Figure 2, a–c; Parysek and Goldman, 1987; Beaulieu *et al.*, 1999b). No other IF proteins (vimentin, NF-H, or keratin) could be detected by immunofluorescence (our unpublished data).

Nondifferentiated PC12 cells were transfected with peripherin-siRNA (see MATERIALS AND METHODS). These preparations were fixed and processed for immunofluores-
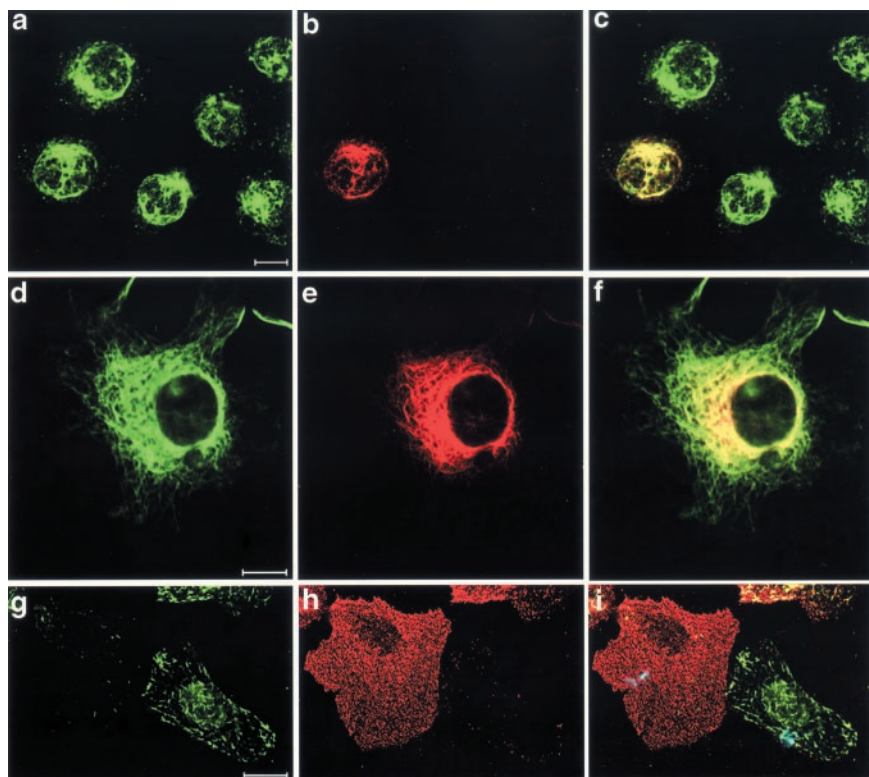
**Figure 2.** Peripherin depletion alters the distribution of NF-M. (a–c) Low magnification view of undifferentiated PC12 cells (grown in CM) double labeled with peripherin (green; a), and NF-M (red; b) antibodies demonstrate that ~30% of cells express NF-M. (d–f) Higher magnification of these NF-M expressing cells reveals that NF-M associates with a subset of peripherin filamentous structures (f; yellow). (g–i) In cells observed ~72 hours after exposure to peripherin-siRNA (i, blue), peripherin levels decrease and NF-M forms non-filamentous punctate structures throughout the cytoplasm. Note the partial reduction in peripherin expression in the cell (*) that does not express NF-M. Size bars a–c, g–i = 10 $\mu$m; Size bar d–f = 5 $\mu$m.

cence with peripherin antibody 24, 48, 72, and 96 h later (Figure 1, c–i). After ~48 h, ~14% (27/200) of the cells exhibited an obvious decrease in the number of long IF structures (Figure 1, f and h). In these same cells, there was an apparent increase in the relative number of particles and squiggles (see, for example, Figure 1, f and h). At 72 h, ~42% (82/220) of cells displayed reduced levels of peripherin: of these ~17% contained only particles and squiggles (partially silenced) and ~83% showed no detectable peripherin (extensively silenced). At ~96 h posttransfection, the number of cells showing decreased peripherin expression had risen to ~61% (121/220); ~20% of these were partially silenced (as seen in Figure 1, f and h), and ~80% were extensively silenced (Figure 1, c–e, g, and i). Identical results were obtained using a second peripherin siRNA (peripherin-siRNA2; as described in MATERIALS AND METHODS; our unpublished data). In contrast, control cells transfected with *X. laevis* lamin B1 siRNA, NF-L siRNA, or mock-transfected (see MATERIALS AND METHODS) showed no detectable alterations in the peripherin IF network at any of the time points (our unpublished data). Under all of these transfection conditions, including peripherin-siRNA, there were no obvious changes in the actin or MT staining patterns as detected by fluorescence microscopy (for example, see Figure 1, f–i). It is also important to note that similar results were obtained using either nonlabeled or fluorescein-labeled siRNAs (Silencer siRNA labeling kit; Ambion).

The medium molecular weight NF subunit (NF-M) requires the presence of NF-L or a type III IF protein, such as peripherin, to coassemble into IF (Parysek *et al.*, 1991; Beaulieu *et al.*, 2000). Therefore, another way to confirm peripherin depletion is to monitor the immunofluorescence pattern of NF-M in peripherin-silenced cells. In the vast majority of these cells observed at 96 h after transfection, NF-M forms punctate nonfilamentous structures distributed throughout the cytoplasm (~98%; 196/200; Figure 2, d–f). Therefore, NF-M is unable to form filamentous structures in the absence of peripherin IF.

Peripherin-silenced undifferentiated cells were morphologically distinct from nontransfected cells on the same coverslips. These cells looked flatter and had fewer processes as determined by combined fluorescence and phase contrast microscopy. To more accurately assess the effects of peripherin-siRNA on PC12 cell morphology, the cellular perimeter, mean cell area, form factor, process domain, and process index were determined (Table 1, a and b; see MATERIALS AND METHODS). In particular, the form factor, process index, and process domain values reflect the roundness of cells, number of processes, and process length, respectively (Kawa *et al.*, 1998; Soll *et al.*, 1988). The resulting data revealed that the overall shape of peripherin-silenced cells and control cells was different as reflected by their increased form factor values and decreased process index and process domain values (Table 1). Therefore, peripherin-depleted cells contained fewer and shorter processes relative to controls.

A more detailed analysis of the morphological features of these cells was carried out by determining the average number and length of cytoplasmic processes as well as the average length of cell bodies (Figure 2 and Table 2a; for definition, see MATERIALS AND METHODS). The average number (2.67 ± 1.77; n = 50) and length (9.91 ± 9.08 $\mu$m; n = 50) of cytoplasmic processes was determined in mock-transfected control cells (Table 2). In contrast, silenced cells had significantly (Student's *t* test; p < 0.002) fewer (1.13 ± 1.98; n = 50) and shorter (6.52 ± 5.56 $\mu$m; n = 50) cytoplasmic processes (Table 2). In addition, the average cell body length was significantly increased (20.22 ± 10.77 $\mu$m; n = 50) in peripherin-depleted cells compared with controls (13.9 ± 6.03 $\mu$m; n = 50) producing a more flattened configuration

**Figure 3.** Peripherin is required for neurite initiation and outgrowth. (a–f) PC12 cells were transfected with peripherin-siRNA, maintained in CM for 72 h, followed by exposure to NGF for 24 h. (a) Peripherin depleted cells (see *) looked fibroblastic in shape and were not able to form neurites. (b and c) The actin (red) networks in these cells were similar to those observed in undifferentiated cells grown in CM (see Figure 1, f and g). Note that nonsilenced cells are capable of forming neurites. (d–f) Higher magnification view of an extensively silenced cell demonstrates the more extensively spread morphology and a lack of neurites. The presence of fluorophore-labeled peripherin-siRNA is indicated in f (blue). For comparison, a periherin (green)-filled neuritic process of an unsilenced cell is shown to the left. Bars, 10 $\mu$m.
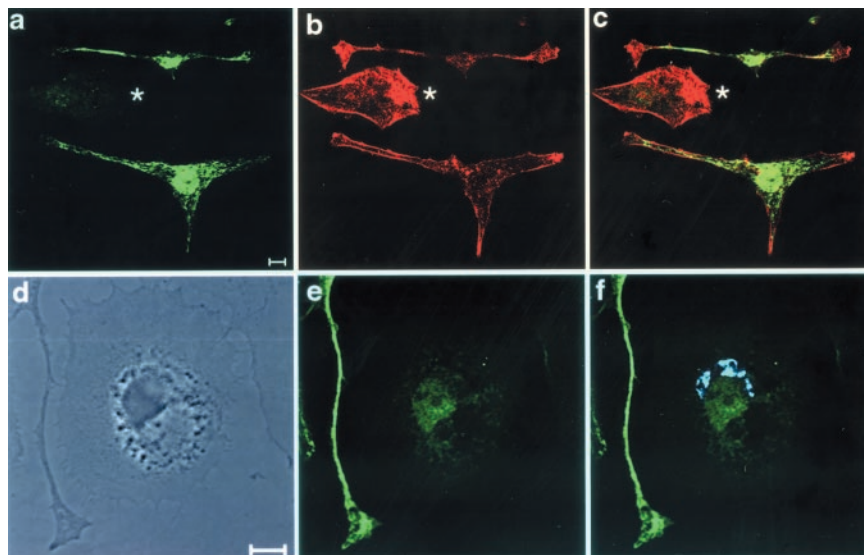
(Figure 1, c, g, and i, and Table 2). In contrast, no significant differences in either the length of cell processes or cell bodies were observed between NF-L siRNA mock- and *X. laevis* B1 siRNA-transfected control groups (our unpublished data).

## Peripherin Is Required for Neurite Initiation and Outgrowth

We previously determined that ~75–80% of the outgrowth of PC12 cell neurites takes place within 24–48 h after exposure to NGF (Figure 1b; 48 h; Helfand *et al.*, 2003). However, the most significant effects of peripherin-siRNA were not observed until ~72–96 h posttransfection (see above). Therefore, to determine whether peripherin is required for neurite initiation and outgrowth, undifferentiated PC12 cells were transfected with peripherin siRNA and maintained in CM for ~72 h. At this time, the medium was replaced with DM containing NGF. After 24 h (~96 h posttransfection), cells were fixed and processed for immunofluorescence. Under these conditions, ~55% (109/200) of the cells showed extensive silencing of peripherin. The morphological features of these cells were indistinguishable from silenced undifferentiated cells (see Figure 1, e, g, and i). The majority (~90%) contained no recognizable peripherin structures (extensively silenced) and others contained a few peripherin particles and squiggles (partially silenced). All of the cells devoid of detectable peripherin were fibroblastic in shape (Figure 3, a–f). Furthermore, there were significant (p <0.005) increases in the form factor and corresponding decreases in the process index and the process domain, suggesting that they were more spheroidal and had fewer and shorter processes (Table 1; see MATERIALS AND METHODS). The average number (0.17 ± 0.52; n = 50) and length (7.16 ± 17.06 $\mu$m; n = 50) of neurites was significantly decreased (p <0.002) compared with the average number (2.2 ± 2.6; n = 75) and length (28.32 ± 22.89 $\mu$m; n = 75) of neurites in control cells (Table 2). Thus, in the absence of peripherin there is a 13 fold reduction in the number of neurites and an ~fourfold reduction in the length of any residual neuritic processes (see Table 2, number and length of neurites). The average cell body length of peripherin siRNA-treated cells (35.51 ± 13.62 $\mu$m) was significantly greater than control cells (16.39 ± 7.88 $\mu$m; Figure 3, d–f, and Table 2), demon-strating that these cells were more extensively flattened. Furthermore, the overall distributions of actin (Figure 3, a–c) and MT (our unpublished data) in peripherin-silenced cells were similar to those in nondifferentiated cells grown in CM (compare with Figure 1, g and i). Together, the results of these experiments suggest that peripherin is required for both the initiation and outgrowth of neurites in PC12 cells.

Live cell observations of peripherin-silenced cells were made to examine any differences in the initiation of growth cones between peripherin depleted and control cells. To this end, PC12 cells were transfected with fluorescein labeled peripherin-siRNA, grown for 72 hours in CM, challenged with NGF and then observed live with phase contrast microcopy at different time periods up to 24 hours. During this period, the silenced cells were easily distinguished from those not transfected with siRNA by their fluorescence and overall morphology. Differences between the silenced and non-silenced cells became evident after 2–4 hours and up to 24 hours after the addition of NGF (DM). Peripherin silenced cells were not able to extend neuritic processes (for example, Video Supplement 1). However, extensive membrane ruffling was seen on silenced cells within 2 hours after the addition of NGF. These ruffling regions were localized in several broad regions at the cell perimeter, but none had the typical fan-shaped appearance of growth cones. Even after 24 hours, this ruffling activity was typically seen in several regions of the cell surface with no dominant region taking on either the role or the morphology of a typical growth cone. In contrast, peripherin containing cells exhibited well-defined growth cones that were actively protruding at the leading edges of extending neurites within a few hours after the addition of NGF (for example, see Video Supplement 1).

## Immunoblot Analyses of the Effects of Peripherin siRNA

Immunoblot analyses of whole cell lysates were performed to further characterize the effects of peripherin-siRNA. To this end, PC12 cells were transfected with peripherin-siRNA and, in parallel cultures, mock transfected. After transfection, the cells were maintained in either CM or DM. In control cells maintained in CM, the levels of peripherin in total cell lysates remained relatively constant for 24–96 h (Figure 4a; CM Mock). The overall levels of peripherin in
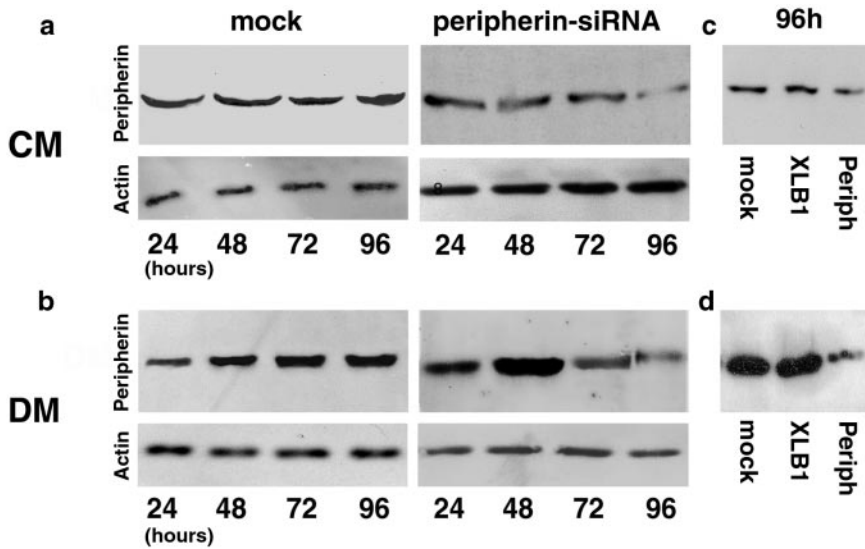
**Figure 4.** Immunoblot analyses of peripherin-siRNA depletion. PC12 were transfected with peripherin-siRNA or mock transfected (mock) and then grown in either CM or DM for 24, 48, 72, or 96 h. (a and b) Samples of the total protein obtained from ~200,000 cells were analyzed by SDS-PAGE and immunoblotting with peripherin and actin antibodies. (a; mock) The amounts of the ~57-kDa peripherin protein present in mock-transfected cells grown in CM remained relatively constant during the time course of the experiment. (a; peripherin-siRNA) However, peripherin-siRNA–treated cells maintained in CM contained ~80% less peripherin by 96 h posttransfection. (b; mock) Increased amounts of peripherin were observed between ~48 and 96 h in mock-transfected cells grown in DM. (b; peripherin-siRNA) Exposure to peripherin-siRNA significantly decreased the levels of peripherin by ~90%. There were no observable effects on the levels of actin under any of these conditions (a and b). (c and d) As a further control, PC12 cells were transfected with either peripherin siRNA (periph), the unrelated *X. laevis* lamin B1(XLB1), or mock transfected with OligofectAMINE (mock). Immunoblot analyses of total cell lysates prepared from PC12 cells grown in either CM (c) or DM (d) at 96 h revealed that only the peripherin-siRNA was able to decrease the levels of peripherin.

siRNA-transfected cells grown in CM seemed unaltered for ~72 h and then decreased to ~20–40% (n = 5) of their original levels by 96 h (Figure 4a; peripherin-siRNA). It should be noted that the amount of peripherin present in mock-transfected cells grown in the presence of NGF increased significantly between ~48 and 96 h (Figure 4b; DM Mock; also see Leonard *et al.*, 1987; Aletta *et al.*, 1988). In comparison, by 96 h the amount of peripherin present in silenced cells grown in DM decreased to ~10–40% of the levels detected at 48 h after transfection with siRNA (n = 5; Figure 4b; peripherin-siRNA). Peripherin-siRNA inhibited the increase in peripherin expression induced by NGF compared with controls (Figure 4b; compare 72–96 h DM, mock with DM, peripherin-siRNA). The results obtained in both CM and DM demonstrate that the effects of peripherin-siRNA are not obvious until ~72–96 h posttransfection, which is consistent with the immunofluorescence results (see above and Figure 1). It should be noted that complete peripherin silencing was never observed by immunoblotting, which is supported by the finding that ~40% of the cells do not seem to be transfected with peripherin-siRNA as determined by immunofluorescence (see above). The levels of actin (Figure 4, a and b) and tubulin (our unpublished data) remained relatively constant under all experimental conditions, confirming the specificity of the effects of peripherin-siRNA. In addition, cells transfected with *X. laevis* lamin B1 siRNA or mock transfected (Figure 4, c and d) showed no differences in peripherin expression in either CM or DM for periods up to 96 h, further confirming the specific effects of peripherin-siRNA.

In addition to peripherin and NF-M, PC12 cells have been reported to express low levels of other types of IF proteins (Franke *et al.*, 1986; Parysek and Goldman, 1987). Therefore, it was of interest to determine whether the expression of these other proteins was altered in silenced and control cells. Immunoblot analyses revealed no differences in the overall levels of vimentin, NF-L, NF-M, NF-H, or keratin under any of the experimental conditions examined (our unpublished data; see MATERIALS AND METHODS). Therefore, other types of IF proteins do not seem to compensate for the loss of peripherin.

### Peripherin Is Also Required for the Maintenance of Neurites

Peripherin seems to be the major cytoskeletal component of differentiated peripheral neurons (Aletta *et al.*, 1989). Therefore, it was also of interest to determine whether it is required for the maintenance of neurites, once they are formed. In a series of experiments, undifferentiated cells were transfected with fluorescein-labeled peripherin-siRNA (see MATERIALS AND METHODS) and then immediately placed in NGF-containing medium (DM) for up to 96 h. The results showed that the majority of peripherin-siRNA–containing cells extended neurites that were morphologically indistinguishable from control cells at ~24 h posttransfection (Figure 5a and Tables 1 and 2). This was expected because the effects of siRNA are not obvious until ~72–96 h posttransfection (see above). However, by ~48 h, some cells containing peripherin-siRNA seemed to possess shorter neurites relative to controls, suggesting a slower rate of neurite outgrowth (Figure 5h). This observation was also supported by a small increase in the form factor, indicating a tendency toward a more rounded contour (Figure 5g and Table 1). In addition, many transfected cells displayed dramatically decreased peripherin staining within their cell bodies, whereas many of their neurites retained peripherin (Figure 5b). After ~96 h, however, most peripherin-silenced cells contained no identifiable peripherin structures, and they looked fibroblastic (Figure 5c). This tendency toward a more fibroblastic shape was also supported by an increase in the form factor and a decrease in the process index and process domain values (Table 1). In control cells after 96 h, the average cell body length was $18.95 \pm 6.56$ $\mu$m (n = 50), and the average number and length of neurites were $2.24 \pm 1.1$ and $62.77 \pm 41.4$ $\mu$m (n = 50), respectively (Table 2). These values were not significantly different from the values obtained from NF-L siRNA transfected cells that had an average cell body length of $23.88 \pm 8.02$ $\mu$m (n = 20), and an
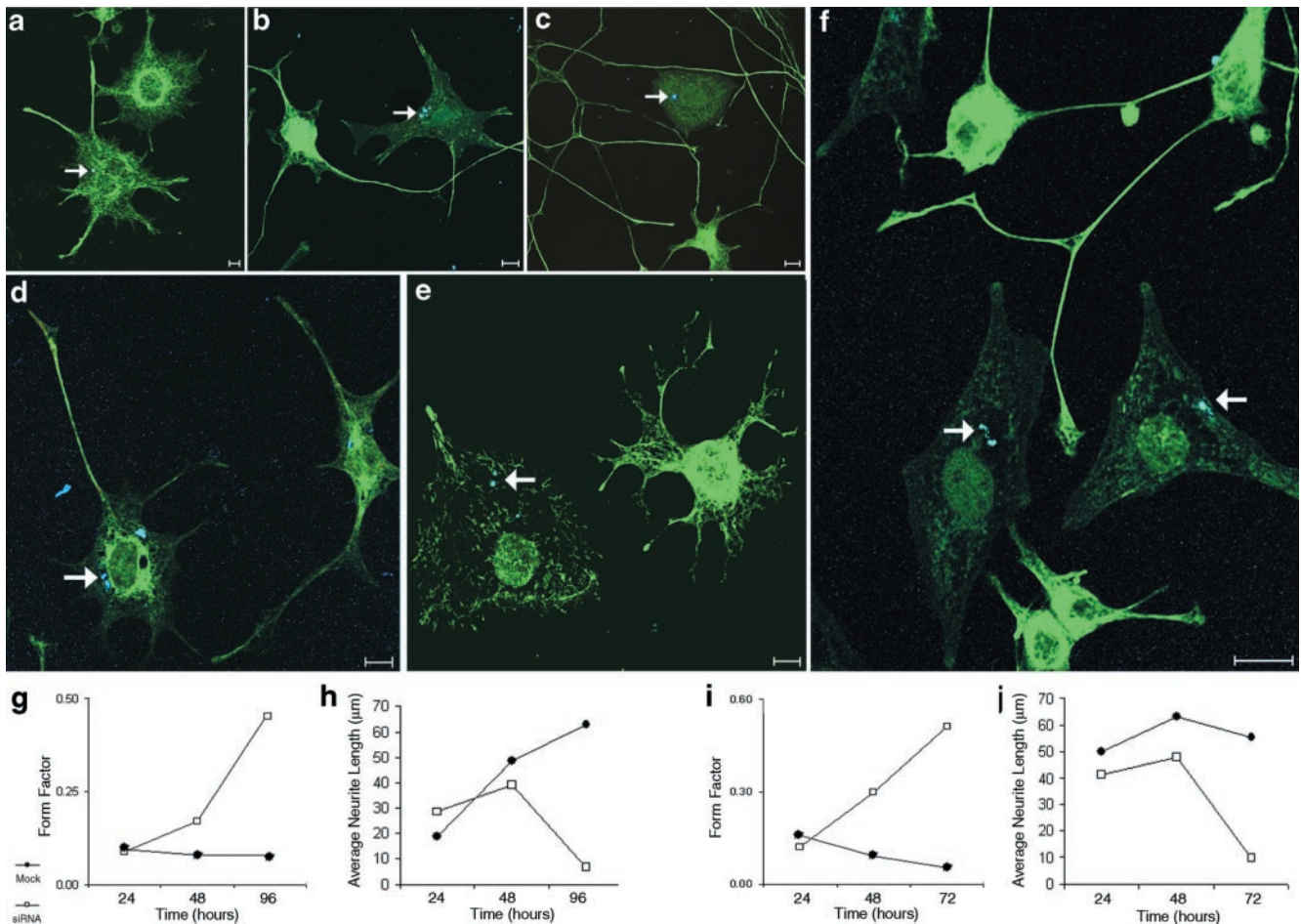
**Figure 5.** Peripherin is required for the maintenance of neurites in PC12 cells. (a–c) PC12 cells were transfected with labeled-peripherin-siRNA (blue, see arrows; FAM see MATERIALS AND METHODS) and were immediately placed in DM for up to 96 h. (a) After 24 h, most transfected PC12 cells contained peripherin and had extended neurites. (b) After ~48 h, many cells showed decreased amounts of peripherin fluorescence within their cell bodies. Interestingly, many of these cells retained peripherin structures within their neuritic processes (see silenced cell in b). (c) By ~72–96 h posttransfection, many silenced cells looked fibroblastic in shape (for comparison, see Figure 1c) and contained no neurites compared with nontransfected cells in the same field of view. (g and h) Analyses of cellular morphology of peripherin-siRNA–treated cells demonstrated significant increases in the form factor and significant decreases in neurite length over time. In contrast, the form factor decreased and neurite length increased in mock-transfected control cells over time. (d–f) Nontransfected PC12 cells were exposed to NGF (DM) for 24 h to induce neurite outgrowth and then transfected with either labeled peripherin-siRNA (blue; see arrows) or mock transfected. Differentiated transfected cells were maintained in DM for 24, 48, and 72 h followed by fixation and staining. (d) Twenty-four hours after transfection, PC12 cells displayed peripherin networks and long neurites. (e) At ~48 h, many cells exhibited a decrease in the total peripherin fluorescence and an increase in the number of peripherin particles throughout the cell body. (f) After ~72 h, most silenced cells looked fibroblastic in shape. (i and j) Peripherin-silenced cells demonstrated significant increases in their form factor and significant decreases in neurite length during the time course of these experiments (j; note that the average neurite length at 24 h reflects the exposure to NGF before transfection). In contrast, the form factor decreased and neurite length increased in mock-transfected control cells (i and j). Bars, 10 $\mu$m.

average number and length of neurites that were 3.50 $\pm$ 2.36 and 54.94.77 $\pm$ 12.99 $\mu$m (n = 20); Table 2). In contrast, direct measurements of peripherin-silenced cells showed a significant increase in the average cell body length (34.82 $\pm$ 14.65 $\mu$m; n = 50), whereas both the number (0.17 $\pm$ 0.42; n = 50) and length (6.89 $\pm$ 15.72 $\mu$m; n = 50) of neurites decreased significantly (Table 2). This emphasizes the dramatic effects of peripherin silencing on the shape and form of differentiated PC12 cells.

To further confirm whether PC12 cells require peripherin for the maintenance of neurites, differentiated cells (treated with NGF for 24 h) were transfected with peripherin-siRNA and maintained in DM for up to an additional 72 h. Under these culture conditions, ~10–20% of the cells were transfected with peripherin-siRNA. None of these showed obvious changes in their immunofluorescence patterns at 24 h posttransfection (Figure 5d). After ~48 h, some cells contained only peripherin particles and squiggles and most of these had only short cytoplasmic processes with no obvious neurites (Figure 5e). Approximately 72 h after transfection, the average number (0.33 $\pm$ 0.61; n = 50) and length (9.48 $\pm$ 16.33 $\mu$m; n = 50) of neurites in silenced cells decreased significantly compared with the average number (2.46 $\pm$ 1.57; n = 50) and length (55.18 $\pm$ 45.5 $\mu$m; n = 50) of neurites in mock-transfected cells (Figure 5, f and j, and Table 2). In addition, the average cell body length (31.12 $\pm$ 13.4 $\mu$m; n =
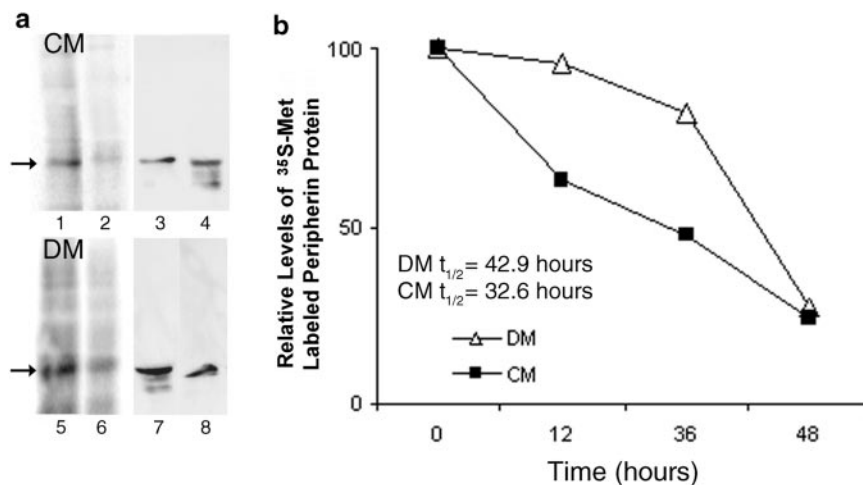
**Figure 6.** Determination of peripherin half-life. Nondifferentiated (grown in CM) and differentiated (grown in DM) PC12 cells were pulse-labeled with [$^{35}$S]methionine for 4 h and then chased with nonradioactive medium for up to 48 h. Intermediate filament-enriched cytoskeletal preparations were made at 0-, 12-, 36-, and 48-h time points and the proteins were separated by SDS-PAGE and analyzed by immunoblotting and autoradiography. The amount of [$^{35}$S]methionine-labeled peripherin present in these preparations at the 48-h time point (a; lanes 2 and 6) was decreased relative to those obtained at the 0 time point (a; lanes 1 and 5). However, the levels of total peripherin protein remained relatively constant between 0 (a; lanes 3 and 7) and 48 h (a; lanes 4 and 8) as determined by immunoblotting. (b) The amounts of labeled peripherin present at 0 h were assigned a value of 100, and later time points were expressed as relative levels of this value. The half-life of peripherin contained within PC12 cells grown in CM and DM was found to be ~33 and ~43 h, respectively. Arrows point to peripherin (57 kDa).

50) of silenced cells was significantly increased relative to controls (17.16 ± 6.25 $\mu$m; n = 50; Table 2). These changes in morphology were reflected as a significant increase in the form factor and corresponding decreases in both the process index and process domains (Figure 5i and Table 1). The results conclusively demonstrate that peripherin is required for the maintenance of neurites.

### The Half-Life of Peripherin in Nondifferentiated and Differentiated PC12 Cells

Immunofluorescence observations showed significant reductions in peripherin-silenced cells as early as 48 h after transfection, which is consistent with the turnover rates that have been determined for other type III IF proteins (McTavish *et al.*, 1983). This is in stark contrast to other results that suggest that the half-life for peripherin is 7–10 d (Troy *et al.*, 1992). Based upon this discrepancy, we felt that it was important to measure the half-life of peripherin in our PC12 cell line by pulse labeling with [$^{35}$S]methionine for 4 h, followed by transfer to nonradioactive medium for different time periods (see MATERIALS AND METHODS). These experiments were carried out on cells grown in either CM or DM for 48 h (see MATERIALS AND METHODS). After labeling, IF-enriched cytoskeletons were prepared and analyzed by SDS-PAGE, immunoblotting, and autoradiography at 0, 24, 36, and 48 h. The results of two separate sets of experiments demonstrated that the total amounts of peripherin present in PC12 IF-enriched cytoskeletal preparations were similar at each time point (Figure 6 a; compare lanes 3 and 4 and 7 and 8). However, the levels of [$^{35}$S]methionine-labeled peripherin fell to 50% of their control values within ~33 h in CM and ~43 h in DM (Figure 6, a, lanes 1 and 2 and 5 and 6; and b). These results are consistent with the time required for peripherin depletion by using siRNA (~72–96 h; see above).

### DISCUSSION

Different cell types are frequently distinguished by their shapes. This is best exemplified in nerve cells, which are remarkably asymmetric due to the presence of long processes such as axons and dendrites. The use of siRNAs to silence the expression of specific proteins in mammalian cells has allowed us to directly address the function of IF in the initiation, outgrowth, and maintenance of neurites. The results of this study clearly demonstrate a significant role for neural IF in both the formation and maintenance of neuritic processes, and thus cell shape. Peripherin-siRNA dramatically decreased the amount of endogenous peripherin in PC12 cells and coincidentally inhibited their ability to extend and maintain neurites. This was demonstrated by the finding that the average length of processes after peripherin silencing was similar to that observed in nondifferentiated cells. In contrast, peripherin-positive cells extended neurites that were at least four to five times longer (Table 2). These observations are also supported by the findings that there are dramatic increases in peripherin expression during the initiation and outgrowth of axons that take place in early developing nervous systems of mammals, amphibians, and fish (Troy *et al.*, 1990b; Gervasi *et al.*, 2000; Undamatla and Szaro, 2001). Similarly, peripherin expression increases significantly during NGF-induced neurite outgrowth in PC12 cells (Parysek and Goldman, 1987; Aletta *et al.*, 1988; Troy *et al.*, 1990a). The levels of peripherin are also up-regulated ~2- to 3-fold during the regrowth of axons after axotomy of mature dorsal root ganglion axons, whereas the levels of NF triplet proteins dramatically decrease (Hoffman and Lasek, 1980; Oblinger *et al.*, 1989a,b).

The inhibition of peripherin expression by using the siRNA approach has numerous advantages over other methods used to inhibit the production of specific proteins in vivo. In this regard, it has been found that siRNA is much more stable and effective in inhibiting expression over longer time periods under normal growth conditions than is the case for antisense probes (Bertrand *et al.*, 2002). For example, in earlier studies, it was found that PC12 cells had to be grown in serum-free medium for 28 d to attain significant decreases in peripherin expression by using the antisense approach (Troy *et al.*, 1992). The half-life for peripherin under these growth conditions was found to be between 7 and 10 d or almost 6 times greater than that reported in this study. Although we cannot explain these discrepancies, it is conceivable that growth in serum-free medium for prolonged periods may have adversely affected the normal expression pattern of peripherin.

The PC12 cell line is an excellent model for studying the function of neural IF in the initiation, outgrowth, and maintenance of neurites, as well as in the overall shape determination of nerve cells (Greene and Tischler, 1976). This is attributable to the finding that all of the cells express one major IF protein, peripherin, which assembles into homopolymer IF in both undifferentiated and differentiated states. Another important property of PC12 cells for these studies is based upon the finding that the expression levels of other IF proteins, such as vimentin and NF, are not detectably increased after the addition of NGF to undifferentiated cells. Even more importantly, the expression of these other IF proteins is not altered to compensate for the dramatic decrease in peripherin expression induced by siRNA. This was best exemplified in the subpopulation of PC12 cells that normally express both peripherin and NF-M. This latter NF protein cannot assemble into IF on its own, but it can coassemble with type III IF such as peripherin (Parysek *et al.*, 1991; Beaulieu *et al.*, 1999a; Figure 2, a–c). Our findings that NF-M only formed nonfilamentous aggregates in peripherin-silenced cells confirmed that there was no compensatory up-regulation of either type III of type IV (NF) proteins (Figure 2, d–f).

Further support for the importance of IF in the determination of cell shape in the nervous system comes from studies of astrocytes. Reactive astrocytes extend long cytoplasmic processes containing three IF proteins; the type III glial fibrillary acidic protein (GFAP) and vimentin, and the type IV protein nestin (Eliasson *et al.*, 1999). Astrocytes from vimentin-null mice contain GFAP IF networks, and there is no obvious alteration in their shape. The same is true for the astrocytes obtained from GFAP-null mice, which express vimentin IF (Pekny *et al.*, 1998; Lepekhin *et al.*, 2001). However, astrocytes obtained from mice that are null for both GFAP and vimentin do not contain endogenous IF, and they approximate a rounded cellular morphology devoid of long cytoplasmic processes. Interestingly, mice null for either vimentin or GFAP can form glial scars in response to brain injury, whereas double knockout (GFAP−/−, vimentin−/−) mice cannot heal brain injuries, resulting in severe intracranial hemorrhaging (Pekny *et al.*, 1999). Together, it seems that some degree of functional overlap exists between vimentin and GFAP, because vimentin seems to be capable of compensating for the loss of GFAP and vice versa. This functional compensation is important to keep in mind when interpreting the results obtained from IF null mice. For example, a recent study reported that peripherin null mice exhibit a significant increase in the type IV homopolymer IF protein $\alpha$-internexin (Lariviere *et al.*, 2002).

The results of the peripherin-siRNA experiments clearly add a new dimension to the many studies documenting the importance of actin and MTs in the structure and function of growth cones and axons, as well as the overall shape of nerve cells (for review, see Letourneau, 1996). In further support of the roles of the different structural forms of IF in these activities, it has recently been demonstrated that IF and their constituent proteins are present throughout all regions of nerve cells, including actin-rich growth cones (Chan *et al.*, 2003; Helfand *et al.*, 2003). Our results strongly suggest that peripherin performs essential functions within these regions, because peripherin-depleted cells cannot form growth cones nor can they extend or maintain neuritic processes.

The relative increases and decreases in the expression patterns of different IF proteins during the development and the regeneration of axons may reflect the unique biochemical, mechanical, and motile properties of individual types of IF. With respect to motility, it has been demonstrated that peripherin and NF containing short filaments (or squiggles) move along MT tracks at rates up to 1–2 $\mu$m/s in association with the molecular motors, kinesin, and cytoplasmic dynein (Yabe *et al.*, 1999, 2000; Prahlad *et al.*, 2000; Shah *et al.*, 2000; Wang *et al.*, 2000; Helfand *et al.*, 2002, 2003). From these observations, it seems that the mechanisms governing the intracellular transport of short NF and peripherin squiggles are not fundamentally different from each other. However, the overall distances traveled by these two types of IF are significantly different. These differences are related to the amount of time that these two types of IF spend moving relative to the time they spend in a stationary phase (i.e., their "pause times"). For short NF, the pause times are ~4 times longer than their peripherin counterparts, and this explains why the net translocation of NF is much slower than peripherin IF (Wang *et al.*, 2000).

The slower movements of NF may be related to their structure and biochemical properties. As mentioned above, type IV NF proteins are composed of three subunits, two of which (NF-H and NF-M) possess extremely long highly charged C-terminal domains thought to be involved in the cross-bridging of NF to other NF, as well as to other cytoskeletal components, such as MT (Miyasaka *et al.*, 1993; Nakagawa *et al.*, 1995). It has been proposed that these cross-bridges account for the increased resistance of NF to mechanical strain (Nakagawa *et al.*, 1995; Leterrier *et al.*, 1996). In contrast, type III IF (e.g., peripherin) have much shorter C termini and are less resistance to mechanical strain (Leterrier *et al.*, 1996). Based on these observations, it is interesting to speculate that the functional significance of the developmentally regulated changes in the expression of different types of neural IF may be related to their specific motile and mechanical properties. For example, during early development, nerve cells require a great deal of plasticity as they undergo the rapid outgrowth and dramatic cell shape changes that typify the transition from immature into mature neurons. Therefore, the early expression of homopolymer type III IF, such as those containing peripherin or vimentin, could provide the cytoskeletal flexibility needed during early development and during the regeneration of injured neurons. In contrast, the overall slower moving, more strain-resistant NF may provide the increased stability necessary to maintain the shape and mechanical integrity of terminally differentiated adult neurons.

## ACKNOWLEDGMENTS

## REFERENCES

Aletta, J.M., R. Angeletti, R. K. Liem, C. Purcell, M. L. Shelanski, and L. A. Greene. (1988). Relationship between the nerve growth factor-regulated clone 73 gene product and the 58-kilodalton neuronal intermediate filament protein (peripherin). J. Neurochem. *51*, 1317–1320.

Aletta, J.M., Shelanski, M.L., and Greene, L.A. (1989). Phosphorylation of the peripherin 58-kDa neuronal intermediate filament protein. Regulation by nerve growth factor and other agents. J. Biol. Chem. *264*, 4619–4627.

Beaulieu, J.M., Jacomy, H., and Julien, J.P. (2000). Formation of intermediate filament protein aggregates with disparate effects in two transgenic mouse models lacking the neurofilament light subunit. J. Neurosci. *20*, 5321–5328.

Beaulieu, J.M., Nguyen, M.D., and Julien, J.P. (1999a). Late onset death of motor neurons in mice overexpressing wild-type peripherin. J. Cell Biol. *147*, 531–544.

Beaulieu, J.M., Robertson, J., and Julien, J.P. (1999b). Interactions between peripherin and neurofilaments in cultured cells: disruption of peripherin assembly by the NF-M and NF-H subunits. Biochem. Cell Biol. *77*, 41–45.

Bertrand, J.R., Pottier, M., Vekris, A., Opolon, P., Maksimenko, A., and Malvy, C. (2002). Comparison of antisense oligonucleotides and siRNAs in cell culture and in vivo. Biochem. Biophys. Res. Commun. *296*, 1000–1004.

Chan, W.K., Yabe, J.T., Pimenta, A.F., Ortiz, D., and Shea, T.B. (2003). Growth cones contain a dynamic population of neurofilament subunits. Cell Motil. Cytoskeleton *54*, 195–207.

Cochard, P., and Paulin, D. (1984). Initial expression of neurofilaments and vimentin in the central and peripheral nervous system of the mouse embryo in vivo. J. Neurosci. *4*, 2080–2094.

Dickson, B.J. (2002). Molecular mechanisms of axon guidance. Science *298*, 1959–1964.

Elbashir, S.M., Harborth, J., Lendeckel, W., Yalcin, A., Weber, K., and Tuschl, T. (2001). Duplexes of 21-nucleotide RNAs mediate RNA interference in cultured mammalian cells. Nature *411*, 494–498.

Eliasson, C., Sahlgren, C., Berthold, C.H., Stakeberg, J., Celis, J.E., Betsholtz, C., Eriksson, J.E., and Pekny, M. (1999). Intermediate filament protein partnership in astrocytes. J. Biol. Chem. *274*, 23996–24006.

Franke, W.W., Grund, C., and Achtstatter, T. (1986). Co-expression of cytokeratins and neurofilament proteins in a permanent cell line: cultured rat PC12 cells combine neuronal and epithelial features. J. Cell Biol. *103*, 1933–1943.

Gervasi, C., Stewart, C.B., and Szaro, B.G. (2000). Xenopus laevis peripherin (XIF3) is expressed in radial glia and proliferating neural epithelial cells as well as in neurons. J. Comp. Neurol. *423*, 512–531.

Greene, L.A., and Tischler, A.S. (1976). Establishment of a noradrenergic clonal line of rat adrenal pheochromocytoma cells which respond to nerve growth factor. Proc. Natl. Acad. Sci. USA *73*, 2424–2428.

Helfand, B.T., Loomis, P., Yoon, M., and Goldman, R.D. (2003). Rapid transport of neural intermediate filament protein. J. Cell Sci. *116*, 2345–2359.

Helfand, B.T., Mikami, A., Vallee, R.B., and Goldman, R.D. (2002). A requirement for cytoplasmic dynein and dynactin in intermediate filament network assembly and organization. J. Cell Biol. *157*, 795–806.

Hesse, M., Magin, T.M., and Weber, K. (2001). Genes for intermediate filament proteins and the draft sequence of the human genome: novel keratin genes and a surprisingly high number of pseudogenes related to keratin genes 8 and 18. J. Cell Sci. *114*, 2569–2575.

Hoffman, P.N., Cleveland, D.W., Griffin, J.W., Landes, P.W., Cowan, N.J., and Price, D.L. (1987). Neurofilament gene expression: a major determinant of axonal caliber. Proc. Natl. Acad. Sci. USA *84*, 3472–3476.

Hoffman, P.N., and Lasek, R.J. (1980). Axonal transport of the cytoskeleton in regenerating motor neurons: constancy and change. Brain Res. *202*, 317–333.

Hoffman, P.N., Thompson, G.W., Griffin, J.W., and Price, D.L. (1985). Changes in neurofilament transport coincide temporally with alterations in the caliber of axons in regenerating motor fibers. J. Cell Biol. *101*, 1332–1340.

Kawa, A., M. Stahlhut, A. Berezin, E. Bock, and V. Berezin. (1998). A simple procedure for morphometric analysis of processes and growth cones of neurons in culture using parameters derived from the contour and convex hull of the object. J. Neurosci. Methods *79*, 53–64.

Laemmli, U.K. (1970). Cleavage of structural proteins during the assembly of the head of bacteriophage T4. Nature. *227*, 680–685.

Lariviere, R.C., Nguyen, M.D., Ribeiro-da-Silva, A., and Julien, J.P. (2002). Reduced number of unmyelinated sensory axons in peripherin null mice. J. Neurochem. 81, 525–532.

Lasek, R.J., Oblinger, M.M., and Drake, P.F. (1983). Molecular biology of neuronal geometry: expression of neurofilament genes influences axonal diameter. Cold Spring Harb. Symp. Quant. Biol. *48*, 731–744.

Leonard, D.G.B., Ziff, E.B., and L. A. Greene. (1987). The detection and characterization of messenger RNAs regulated by nerve growth factor in PC12 cells. Mol. Cell. Biol. *7*, 3156–3167.

Leonard, D.G.B., Gorham, J.D., Cole, P., Green, L.A., and Ziff, E.B. (1988). A nerve growth factor-regulated messenger RNA encodes a new intermediate filament protein. J. Cell Biol. *106*, 181–193.

Lepekhin, E.A., Eliasson, C., Berthold, C.H., Berezin, V., Bock, E., and Pekny, M. (2001). Intermediate filaments regulate astrocyte motility. J. Neurochem. *79*, 617–625.

Leterrier, J.F., Kas, J., Hartwig, J., Vegners, R., and Janmey, P.A. (1996). Mechanical effects of neurofilament cross-bridges. Modulation by phosphorylation, lipids, and interactions with F-actin. J. Biol. Chem. *271*, 15687–15694.

Letourneau, P.C. (1996). The cytoskeleton in nerve growth cone motility and axonal pathfinding. Perspect. Dev. Neurobiol. *4*, 111–123.

Leung, C.L., Flores, R.L., and Liem, R.K. (1998). The complexity of intermediate filaments in the nervous system. Subcell. Biochem. *31*, 497–526.

McTavish, C.F., Nelson, W.J., and Traub, P. (1983). The turnover of vimentin in Ehrlich ascites tumour cells. FEBS Lett. *154*, 251–256.

Miyasaka, H., Okabe, S., Ishiguro, K., Uchida, T., and N. Hirokawa. (1993). Interaction of the tail domain of high molecular weight subunits of neurofilaments with the COOH-terminal region of tubulin and its regulation by tau protein kinase II. J. Biol. Chem. *268*, 22695–22702.

Mueller, B.K. (1999). Growth cone guidance: first steps towards a deeper understanding. Annu. Rev. Neurosci. *22*, 351–388.

Nakagawa, T., Chen, J., Zhang, Z., Kanai, Y., and Hirokawa, N. (1995). Two distinct functions of the carboxyl-terminal tail domain of NF-M upon neurofilament assembly: cross-bridge formation and longitudinal elongation of filaments. J. Cell Biol. *129*, 411–429.

Oblinger, M.M., Szumlas, R.A., Wong, J., and Liuzzi, F.J. (1989a). Changes in cytoskeletal gene expression affect the composition of regenerating axonal sprouts elaborated by dorsal root ganglion neurons in vivo. J. Neurosci. *9*, 2645–2653.

Oblinger, M.M., Wong, J., and Parysek, L.M. (1989b). Axotomy-induced changes in the expression of a type III neuronal intermediate filament gene. J. Neurosci. *9*, 3766–3775.

Parysek, L.M., and Goldman, R.D. (1987). Characterization of intermediate filaments in PC12 cells. J. Neurosci. *7*, 781–791.

Parysek, L.M., McReynolds, M.A., Goldman, R.D., and Ley, C.A. (1991). Some neural intermediate filaments contain both peripherin and the neurofilament proteins. J. Neurosci. Res. *30*, 80–91.

Pekny, M., Eliasson, C., Chien, C.L., Kindblom, L.G., Liem, R., Hamberger, A., and Betsholtz, C. (1998). GFAP-deficient astrocytes are capable of stellation in vitro when cocultured with neurons and exhibit a reduced amount of intermediate filaments and an increased cell saturation density. Exp. Cell Res. *239*, 332–343.

Pekny, M., Johansson, C.B., Eliasson, C., Stakeberg, J., Wallen, A., Perlmann, T., Lendahl, U., Betsholtz, C., Berthold, C.H., and Frisen, J. (1999). Abnormal reaction to central nervous system injury in mice lacking glial fibrillary acidic protein and vimentin. J. Cell Biol. *145*, 503–514.

Portier, M.M., Brachet, P., Croizat, B., and Gros, F. (1983a). Regulation of peripherin in mouse neuroblastoma and rat PC 12 pheochromocytoma cell lines. Dev. Neurosci. *6*, 215–226.

Portier, M.M., de Nechaud, B., and Gros, F. (1983b). Peripherin, a new member of the intermediate filament protein family. Dev. Neurosci. *6*, 335–344.

Prahlad, V., Helfand, B.T., Langford, G.M., Vale, R.D., and Goldman, R.D. (2000). Fast transport of neurofilament protein along microtubules in squid axoplasm. J. Cell Sci. *113*, 3939–46.

Prahlad, V., Yoon, M., Moir, R.D., Vale, R.D., and Goldman, R.D. (1998). Rapid movements of vimentin on microtubule tracks: kinesin-dependent assembly of intermediate filament networks. J. Cell Biol. *143*, 159–170.

Shah, J.V., Flanagan, L.A., Janmey, P.A., and Leterrier, J.F. (2000). Bidirectional translocation of neurofilaments along microtubules mediated in part by dynein/dynactin. Mol. Biol. Cell. *11*, 3495–3508.

Shi, Y. (2003). Mammalian RNAi for the masses. Trends Genet. *19*, 9–12.

Soll, D.R., Voss, E., Varnum-Finney, B., and Wessels, D. (1988). "Dynamic Morphology System": a method for quantitating changes in shape, pseudopod formation, and motion in normal and mutant amoebae of *Dictyostelium discoideum*. J. Cell Biochem. *37*, 177–192.

Starger, J.M., and Goldman, R.D. (1977). Isolation and preliminary characterization of 10-nm filaments from baby hamster kidney (BHK-21) cells. Proc. Natl. Acad Sci. USA *74*, 2422–2426.

Towbin, H., Staehelin, T., and Gordon, J. (1979). Electrophoretic transfer of proteins from polyacrylamide gels to nitrocellulose sheets: procedure and some applications. Proc. Natl. Acad. Sci. USA *76*, 4350–4354.

Troy, C.M., Brown, K., Greene, L.A., and Shelanski, M.L. (1990a). Ontogeny of the neuronal intermediate filament protein, peripherin, in the mouse embryo. Neuroscience *36*, 217–237.

Troy, C.M., Greene, L.A., and Shelanski, M.L. (1992). Neurite outgrowth in peripherin-depleted PC12 cells. J. Cell Biol. *117*, 1085–1092.

Troy, C.M., Muma, N.A., Greene, L.A., Price, D.L., and Shelanski, M.L. (1990b). Regulation of peripherin and neurofilament expression in regenerating rat motor neurons. Brain Res. *529*, 232–238.

Undamatla, J., and Szaro, B.G. (2001). Differential expression and localization of neuronal intermediate filament proteins within newly developing neurites in dissociated cultures of Xenopus laevis embryonic spinal cord. Cell Motil. Cytoskeleton *49*, 16–32.

Wang, L., Ho, C.L., Sun, D., Liem, R.K., and Brown, A. (2000). Rapid movement of axonal neurofilaments interrupted by prolonged pauses. Nat. Cell Biol. *2*, 137–141.

Yabe, J.T., Jung, C., Chan, W.K., and Shea, T.B. (2000). Phospho-dependent association of neurofilament proteins with kinesin in situ. Cell Motil. Cytoskeleton. *45*, 249–262.

Yabe, J.T., Pimenta, A., and Shea, T.B. (1999). Kinesin-mediated transport of neurofilament protein oligomers in growing axons. J. Cell Sci. *112*, 3799–3814.

Yoon, K.H., Yoon, M., Moir, R.D., Khuon, S., and Goldman, R.D. (2001). Insights into the dynamic properties of keratin intermediate filaments in living epithelial cells. J. Cell Biol. *153*, 503–516.